

# Joint Power and Spectrum Orchestration for D2D Semantic Communication Underlying Energy-Efficient Cellular Networks

Le Xia, *Member, IEEE*, Yao Sun, *Senior Member, IEEE*, Haijian Sun, *Senior Member, IEEE*, Rose Qingyang Hu, *Fellow, IEEE*, Dusit Niyato, *Fellow, IEEE*, and Muhammad Ali Imran, *Fellow, IEEE*

**Abstract**—Semantic communication (SemCom) has been recently deemed a promising next-generation wireless technique to enable efficient spectrum savings and information exchanges, thus naturally introducing a novel and practical network paradigm where cellular and device-to-device (D2D) SemCom approaches coexist. Nevertheless, the involved wireless resource management becomes complicated and challenging due to the unique semantic performance measurements and energy-consuming semantic coding mechanism. To this end, this paper jointly investigates power control and spectrum reuse problems for energy-efficient D2D SemCom cellular networks. Concretely, we first model the user preference-aware semantic triplet transmission and leverage a novel metric of semantic value to identify the semantic information importance conveyed in SemCom. Then, we define the additional power consumption from semantic encoding in conjunction with basic power amplifier dissipation to derive the overall system energy efficiency (semantics/Joule). Next, we formulate an energy efficiency maximization problem for joint power and spectrum allocation subject to several SemCom-related and practical constraints. Afterward, we propose an optimal resource management solution by employing the fractional-to-subtractive problem transformation and decomposition while developing a three-stage method with theoretical analysis of its optimality guarantee and computational complexity. Numerical results demonstrate the adequate performance superiority of our proposed solution compared with different benchmarks.

**Index Terms**—Device-to-device semantic communication, energy efficiency, power allocation, spectrum reuse.

## I. INTRODUCTION

RECENT advances in semantic communication (SemCom) have shown great potential in enabling efficient information interaction and high resource utilization, promising to significantly relieve the scarcity of wireless resources in next-generation wireless cellular networks [1]. As a Shannon-beyond communication paradigm, SemCom concentrates upon accurately capturing the true meaning true meanings implied in source messages, rather than merely transmitting bits [2].

Le Xia, Yao Sun (*Corresponding author: Yao Sun.*), and Muhammad Ali Imran are with the James Watt School of Engineering, University of Glasgow, Glasgow G12 8QQ, UK (e-mail: xiale1995@outlook.com; {Yao.Sun, Muhammad.Imran}@glasgow.ac.uk).

Haijian Sun is with the School of Electrical and Computer Engineering, University of Georgia, Athens, GA 30602, USA (e-mail: hsun@uga.edu).

Rose Qingyang Hu is with the Bradley Department of Electrical and Computer Engineering, Virginia Tech, Blacksburg, VA 24061, USA (e-mail: rosehu@vt.edu).

Dusit Niyato is with the College of Computing and Data Science, Nanyang Technological University, Singapore 639798 (e-mail: dniyato@ntu.edu.sg).

Particularly benefiting from the prosper advancement of artificial intelligence (AI), many state-of-the-art sophisticated deep learning (DL) algorithms are expected to be embedded into wireless terminal devices, and such integration enables SemCom to achieve core semantic delivery for various high-quality, large-capacity, and multimodal services, including typical multimedia content (e.g., text [3], image [4], and video streaming [5]) and AI-generated content (AIGC) [6].

Notably, most of the related works have focused on simple and practical device-to-device (D2D) SemCom scenarios, where the DL-driven semantic encoder and semantic decoder are deployed in the transmitter and receiver, respectively. Xie *et al.* [3] devised a Transformer-based SemCom transceiver for reliable text transmission, which was then upgraded to be lightweight in [7]. In [8], Weng *et al.* employed an attention mechanism-enabled squeeze-and-excitation network for transmitting speech signals in SemCom. Besides, Xia *et al.* [6] developed a generative AI-integrated end-to-end SemCom framework in a cloud-edge-mobile design for multimodal AIGC provisioning. From all these studies, notice that efficient semantic inference and recovery must be based on equivalent background knowledge and jointly trained semantic coding models. Keep this in mind, it is envisioned that D2D SemCom underlying cellular networks will become a very common and versatile architecture. On one hand, the D2D SemCom links is capable of reusing the subcarriers of cellular SemCom links to further improve the spectrum utilization. On the other hand, the knowledge sharing and joint model training in SemCom can be easier to implement and coordinate in practice, as the transceivers in each D2D pair are usually in close proximity to each other [9]. Therefore, the D2D SemCom approach renders a more flexible, targeted, and economical pathway to unlocking the full potential of SemCom cellular networks.

As a matter of fact, there have been some noteworthy technical works addressing a variety of challenges in semantics-aware wireless networks. Proceeding the metrics in [3], Yan *et al.* [10] exploited the semantic spectral efficiency optimization-based channel assignment. Zhang *et al.* [11] proposed a deep reinforcement learning-based dynamic resource allocation scheme to optimize the long-term transmission efficiency in task-oriented SemCom networks. Likewise, the integration of energy harvesting and SemCom in resource-constrained Internet of Things systems was considered by Sang *et al.* [12] for power transfer and channel allocation. In addition, Xia *et al.* [13] developed a best mode selection strategy with joint

optimization of user association and bandwidth allocation for hybrid semantic/bit communication networks. Moreover, Su *et al.* [14] explored the semantic access problem in D2D vehicular networks, and Yang *et al.* [15] adopted a probability graph alongside a rate-splitting scheme to assign limited resources to SemCom users for improving the energy efficiency.

Nevertheless, there is still a lack of relevant investigations from an energy-efficient networking perspective on the more general and practical scenario of *D2D SemCom Networks* (D2D-SCNs), in which cellular SemCom users and D2D SemCom user pairs coexist. In full view of its novel paradigm, our main task lies in seeking the optimal strategy for two closely relevant and coupled wireless resource management issues of power control and spectrum reuse in it. Unfortunately, solutions to conventional communication scenarios cannot be directly applied due to the new focus of semantic delivery and the new requirements of semantic coding in SemCom. To be more specific, SemCom entails more circuit power consumption for semantic coding, while SemCom users expect only high semantic fidelity in line with their individual semantic service preferences. Especially when considering energy-efficient large-scale D2D-SCNs, how to maximize the overall system energy efficiency (*semantics-per-Joule*) by trading off energy consumption and acquired semantic-level performance at multiple cellular and D2D SemCom users should be rather complicated and challenging. In summary, we are encountering three fundamental challenges in D2D-SCNs as follows:

- *Challenge 1: How to measure the semantic-level performance for each wireless SemCom link?* Differing from traditional bit-oriented communication, the semantic-level performance needs to be carefully characterized in SemCom due to its sole focus on meaning delivery. Especially noting that users may have personal preferences and background knowledge for varying SemCom services, even the same source information transmitted from different SemCom users could represent different semantic importance, which raises the first nontrivial point.
- *Challenge 2: How to adequately consider the semantic coding process when defining the new energy efficiency model in SemCom?* Owing to unique semantic encoding/decoding requirements, additional power for information extraction and inference is consumed in SemCom-enabled transceivers. Besides, system performance per unit of consumed energy should be measured at the semantic level, as emphasized in Challenge 1, thus requiring a new definition of energy efficiency for D2D-SCN.
- *Challenge 3: How to achieve the best energy-efficient D2D-SCN through wireless resource optimization?* Clearly, power allocation and spectrum reuse are two key issues in resource utilization that can significantly affect the achievable semantic performance for each SemCom user. If aiming at maximizing overall energy efficiency, besides practical constraints such as limited power control and single-subchannel-reusing requirement, ample quality of semantic experience must also be taken into account in resource optimization for each cellular user (CUE) and D2D user (DUE), thereby posing the third difficulty.

In response to the above challenges, in this paper, we propose an optimal joint power allocation and spectrum reuse strategy for energy efficiency maximization in D2D-SCNs taking into account the unique SemCom characteristics. Both theoretical analysis and numerical results showcase the performance superiority of the proposed solution in terms of energy efficiency, semantic performance, and total power consumption compared with two different benchmarks. In a nutshell, our main contributions are summarized as follows:

- We first construct a semantic triplet transmission model for each SemCom-enabled CUE and DUE, which is tightly coupled with the two fundamental problems of power allocation and spectrum reuse. Particularly, considering personal preferences for different SemCom services, we then leverage a novel performance metric called semantic value to identify the semantic information importance of semantic triplets conveyed by each SemCom user, which addresses the *Challenge 1*.
- We carefully define the power consumption occurred during the semantic encoding process in conjunction with basic power amplifier dissipation to derive the overall energy efficiency of D2D-SCN. Afterward, we mathematically formulate a joint power and spectrum orchestration problem to maximize the energy efficiency subject to several SemCom-related and practical system constraints. The contribution directly addresses *Challenge 2*.
- We develop an efficient resource management solution to address the optimization problem, and its optimality is theoretically proved by two propositions. Specifically, a fractional-to-subtractive transformation approach is employed to decompose the complex primal problem into multiple tractable subproblems. Then, a three-stage method is devised to solve each subproblem with polynomial-time computational complexity. In each iteration of the solution, the first and second stages are to obtain the optimal power allocation policy and the third stage is to finalize the optimal spectrum reusing pattern. In this way, *Challenge 3* is finally well tackled.

The remainder of this paper is organized as follows. Section II first introduces the system model of D2D-SCN and formulates the associated energy efficiency maximization problem. Then, we illustrate the proposed optimal power allocation and spectrum reusing strategy in Section III. Numerical results are demonstrated and discussed in Section IV, followed by the conclusions in Section V.

## II. SYSTEM MODEL AND PROBLEM FORMULATION

In this section, the considered D2D-SCN scenario is first elaborated along with the semantic performance measurement and semantic coding-related energy efficiency model. Then, the corresponding resource optimization problem is presented.

### A. D2D-SCN Scenario

Consider a single-cell D2D-SCN scenario as shown in Fig. 1, where  $M$  CUEs and  $N$  ( $N \leq M$ ) pairs of DUEs are capable of performing  $K$  different wireless SemCom services

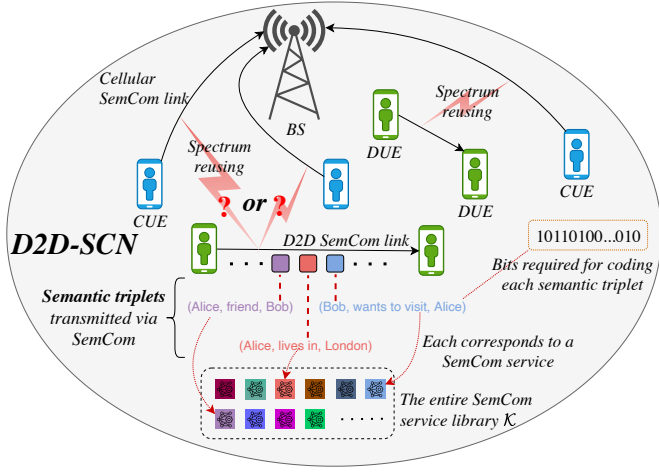


Fig. 1. The D2D-SCN with multiple SemCom-enabled CUEs and DUEs.

based on a SemCom service library  $\mathcal{K} = \{1, 2, \dots, K\}$ .<sup>1</sup> Each CUE  $i \in \mathcal{M} = \{1, 2, \dots, M\}$  is assumed to be pre-allocated an orthogonal uplink subchannel with equal channel bandwidth  $W$  to execute SemCom with its remote receiver. Besides, each DUE  $j \in \mathcal{N} = \{1, 2, \dots, N\}$  is allowed to reuse the subchannel of only one CUE for SemCom service provisioning, and to preserve generality, the subchannel of each CUE can be reused by at most one DUE. Let  $\alpha_{i,j} \in \{0, 1\}$  denote the spectrum reuse indicator, where  $\alpha_{i,j} = 1$  represents that DUE  $j$  reuses the subchannel of CUE  $i$ , and  $\alpha_{i,j} = 0$  otherwise. Furthermore, assuming that each CUE and each DUE have their respective maximum transmit power, denoted by  $P_{max}^C$  and  $P_{max}^D$ .

### B. Channel Model and Semantic Performance Measurement

In the data dissemination model, the channel power gain between CUE  $i$  and the BS, the gain between DUE  $j$  and the BS, the gain between the transmitter and the receiver at DUE  $j$ , and the gain between each CUE  $i$  and each DUE  $j$  are first denoted as  $G_{i,B}$ ,  $G_{j,B}$ ,  $G_j^D$ , and  $G_{i,j}$ , respectively. With the transmit power of each CUE  $i$  and DUE  $j$  denoted as  $P_i^C$  and  $P_j^D$ , considering all potential spectrum reusing cases, the achievable instantaneous bit rate at the uplink of CUE  $i$  is

$$r_i^C = W \log_2 \left( 1 + \frac{P_i^C G_{i,B}}{\delta^2 + \sum_{j \in \mathcal{N}} \alpha_{i,j} P_j^D G_{j,B}} \right), \quad (1)$$

and the achievable instantaneous bit rate at DUE  $j$  is

$$r_j^D = W \log_2 \left( 1 + \frac{P_j^D G_j^D}{\delta^2 + \sum_{i \in \mathcal{M}} \alpha_{i,j} P_i^C G_{i,j}} \right), \quad (2)$$

where  $\delta^2$  is the noise power.

As for the SemCom model, a concept of *semantic triplet* is introduced to represent the interpretable relationship between two specific semantic entities implied in source information [17]–[19], and its typical expression is (*Entity-A*,

<sup>1</sup>Here, different SemCom services can be deemed different semantic delivery tasks, each based on a certain modality (e.g., text or image) associated with a specific knowledge domain (e.g., sports or music) [2], [16].

*Relationship, Entity-B*), for instance, (Alice, friend, Bob), as depicted in Fig. 1. In this work, we assume that different SemCom services randomly arrive at CUEs and DUEs [20], and the source information corresponding to arbitrary SemCom service needs to be fed into the semantic encoder to extract multiple semantic triplets.<sup>2</sup> Afterward, each semantic triplet is encoded to  $L$  bits on average by each user's channel encoder and transmitted to the wireless channel [19]. As such, the total number of semantic triplets that can be transmitted by CUE  $i$  and DUE  $j$  per second are given by  $\lfloor r_i^C / L \rfloor$  and  $\lfloor r_j^D / L \rfloor$ , respectively.

Meanwhile, it is noticed that different CUEs and DUEs may have different personal preferences for these  $K$  SemCom services, resulting in varying proportions of the number of semantic triplets based on different SemCom services during transmission. Without the loss of generality, we consider that the SemCom service popularity at each CUE and DUE follows the Zipf distribution [21],<sup>3</sup> and all CUEs and DUEs are assumed to have identical semantic encoding capabilities for any source information. In this way, the expected number of semantic triplets transmitted for SemCom service  $k \in \mathcal{K}$  at CUE  $i$  per second is calculated by  $\lfloor r_i^C / L \rfloor \cdot (u_{i,k}^C)^{-\beta_i^C} / \sum_{e \in \mathcal{K}} e^{-\beta_i^C}$ , where  $\beta_i^C$  ( $\beta_i^C \geq 0$ ) is the skewness of CUE  $i$ 's Zipf distribution and  $u_{i,k}^C$  is its popularity ranking for SemCom service  $k$ .<sup>4</sup> Likewise, the expected number of semantic triplets transmitted for SemCom service  $k$  at DUE  $j$  per second is  $\lfloor r_j^D / L \rfloor \cdot (u_{j,k}^D)^{-\beta_j^D} / \sum_{e \in \mathcal{K}} e^{-\beta_j^D}$ , where  $u_{j,k}^D$  and  $\beta_j^D$  are DUE  $j$ 's popularity ranking for SemCom service  $k$  and the skewness of its Zipf distribution, respectively.

Naturally, transmitting the higher-ranked semantic triplets contributes more valuable semantic information for each SemCom receiver. Inspired by this, we employ a performance metric called *semantic value* proposed in [19] to measure the semantic information importance of semantic triplets with different rankings.<sup>5</sup> Based on its measurement mechanism, the aforementioned Zipf distribution is leveraged again to compute the semantic value of each ranked semantic triplet of SemCom service  $k$  at CUE  $i$  and DUE  $j$  as  $(u_{i,k}^C)^{-\beta_i^C}$  and  $(u_{j,k}^D)^{-\beta_j^D}$ , respectively. Consequently, if taking into account the semantic triplets of all  $K$  SemCom services, we can obtain the semantic value transmitted by CUE  $i$  per second as follows:

$$V_i^C = \left\lfloor \frac{r_i^C}{L} \right\rfloor \sum_{u_{i,k}^C \in \mathcal{K}} \frac{(u_{i,k}^C)^{-2\beta_i^C}}{\sum_{e \in \mathcal{K}} e^{-\beta_i^C}} \triangleq \theta_i^C \left\lfloor \frac{r_i^C}{L} \right\rfloor, \quad (3)$$

<sup>2</sup>This assumption is justified since core semantic information can be extracted by state-of-the-art DL models from multimedia services (e.g., text [3], image [4], and video [5]) to draw the semantic knowledge graph, which can be decomposed into multiple semantic triplets. In other words, it is reasonable that source information in any format can be transferred in units of semantic triplets for SemCom service provisioning.

<sup>3</sup>Other known probability distributions can also be adopted without changing the remaining modeling and solution.

<sup>4</sup>The SemCom service popularity ranking of each user can be analyzed and estimated based on its historical messaging records [16], [22], [23].

<sup>5</sup>Note that other similar semantic-level metrics can also be applied here without changing the remaining modeling and solution.

and the semantic value transmitted by DUE  $j$  per second is

$$V_j^D = \left\lfloor \frac{r_j^D}{L} \right\rfloor \sum_{u_{j,k}^D \in \mathcal{K}} \frac{(u_{j,k}^D)^{-2\beta_j^D}}{\sum_{e \in \mathcal{K}} e^{-\beta_j^D}} \triangleq \theta_j^D \left\lfloor \frac{r_j^D}{L} \right\rfloor, \quad (4)$$

where the two parameters  $\theta_i^C$  and  $\theta_j^D$  are defined for brevity. Clearly, the overall semantic value transmitted by all CUEs and DUEs in the D2D-SCN per second is given by  $V^{total} = \sum_{i \in \mathcal{M}} V_i^C + \sum_{j \in \mathcal{N}} V_j^D$ .

### C. Energy Efficiency Model of SemCom Systems

In this work, we focus on the overall power consumption including the contributions of the unique semantic encoding circuit module and the transmit power amplifier at each SemCom user. Different from conventional models focusing on the circuit power consumption on bit processing [24] or antenna controlling [25], the power consumption in the SemCom-enabled user devices is primarily considered to be related to the computing for each semantic triplet during the semantic encoding process.<sup>6</sup> This is justified because the relationship between two information entities in each semantic triplet necessarily requires a certain computing power to be accurately identified, reasoned and interpreted, and such semantic encoding tasks are sometimes accomplished by sophisticated DL algorithms-integrated circuit module [26].

Now, suppose that all CUEs and DUEs have fixed circuit power consumption, denoted by  $P^{enc}$ , to encode each semantic triplet, and assume that all semantic triplets generated by the semantic encoder per second are fully transmitted out. Hence, the total circuit power consumption (in *Joule/s*) for semantic encoding in the D2D-SCN can be estimated by

$$E^s = P^{enc} \left( \sum_{i \in \mathcal{M}} \left\lfloor \frac{r_i^C}{L} \right\rfloor + \sum_{j \in \mathcal{N}} \left\lfloor \frac{r_j^D}{L} \right\rfloor \right). \quad (5)$$

Besides, most of related works also consider the power dissipation at power amplifiers of transmitters [9], [24], [27], which has been widely recognized as one of the energy loss sources in present wireless networks. As such, we define the power amplifier inefficiency coefficient as  $\xi$  ( $\xi \geq 1$ ), which is a constant associated with the transmit power of each CUE and DUE. As such, the total power consumption for semantic triplet transmission in the D2D-SCN is obtained from

$$E^t = \xi \left( \sum_{i \in \mathcal{M}} P_i^C + \sum_{j \in \mathcal{N}} P_j^D \right). \quad (6)$$

Accordingly, the total power consumption at all CUEs and DUEs is  $E^{total} = E^s + E^t$ . Since the semantic value performance becomes the sole focus of SemCom, we define the energy efficiency of D2D-SCN as the overall semantic value successfully transferred to the SemCom-enabled receiver per Joule of energy consumed on average, given by

$$\eta_{EE} = \frac{V^{total}}{E^{total}} = \frac{\sum_{i \in \mathcal{M}} V_i^C + \sum_{j \in \mathcal{N}} V_j^D}{E^s + E^t}. \quad (7)$$

<sup>6</sup>Note that the circuit power consumption of semantic decoding at the receiver side is not considered as it is fixed, whereas the transmit power is of main concern in this work.

### D. Problem Formulation

For ease of illustration, we first define three variable sets  $\mathbf{P}^C = \{P_i^C \mid i \in \mathcal{M}\}$ ,  $\mathbf{P}^D = \{P_j^D \mid j \in \mathcal{N}\}$ , and  $\alpha = \{\alpha_{i,j} \mid i \in \mathcal{M}, j \in \mathcal{N}\}$  that consist of all possible indicators pertinent to power allocation and spectrum reusing, respectively. Without loss of generality, the objective is to maximize the energy efficiency  $\eta_{EE}$  of D2D-SCN by jointly optimizing  $(\mathbf{P}^C, \mathbf{P}^D, \alpha)$ , and subject to SemCom-related requirements alongside several practical system constraints. The problem is formulated as follows:

$$\mathbf{P0} : \max_{\mathbf{P}^C, \mathbf{P}^D, \alpha} \eta_{EE} \quad (8)$$

$$\text{s.t. } V_i^C \geq V_{min}^C, \quad \forall i \in \mathcal{M}, \quad (8a)$$

$$V_j^D \geq V_{min}^D, \quad \forall j \in \mathcal{N}, \quad (8b)$$

$$0 \leq P_i^C \leq P_{max}^C, \quad \forall i \in \mathcal{M}, \quad (8c)$$

$$0 \leq P_j^D \leq P_{max}^D, \quad \forall j \in \mathcal{N}, \quad (8d)$$

$$\sum_{j \in \mathcal{N}} \alpha_{i,j} \leq 1, \quad \forall i \in \mathcal{M}, \quad (8e)$$

$$\sum_{i \in \mathcal{M}} \alpha_{i,j} = 1, \quad \forall j \in \mathcal{N}, \quad (8f)$$

$$\alpha_{i,j} \in \{0, 1\}, \quad \forall (i, j) \in \mathcal{M} \times \mathcal{N}. \quad (8g)$$

Constraints (8a) and (8b) guarantee the minimum semantic value achieved at each CUE and DUE, respectively. Similarly, constraints (8c) and (8d) limit the maximum transmit power for each CUE and DUE, respectively. Constraint (8e) represents that the subchannel of each CUE can be shared by at most one DUE, while constraint (8f) requires that each DUE can reuse only one subchannel of an existing CUE. Finally, constraint (8g) characterizes the binary properties of  $\alpha$ .

Carefully examining **P0**, it can be observed that the optimization is quite challenging to be solved straightforwardly due to several intractable mathematical obstacles. First, **P0** involves both continuous and discrete variables, leading to an obvious NP-hard problem. Besides, the expression of the objective function  $\eta_{EE}$  is quite complicated alongside the constraints (8a) and (8b), which is nonconvex and thus generally requires a high-complexity solution procedure. Therefore, we propose an efficient power allocation and spectrum reusing strategy in the next section to reach the optimality of **P0**.

### III. OPTIMAL RESOURCE ALLOCATION FOR D2D-SCNS

In this section, we illustrate how to design our optimal resource allocation algorithm to cope with the energy efficiency optimization problem in the D2D-SCN. As depicted in Fig. 2, the primal problem **P0** is first transformed, without losing optimality, from its original fractional form into an equivalent subtractive form (referring to **P1** in Subsection III-A) by employing the Dinkelbach's method [28]. Then, **P1** is decomposed into multiple subproblems that will be solved in an iterative fashion, and in each iteration, we specially devise a three-stage method. In the first and the second stage, we construct  $U = M \times N$  subproblems (referring to **P2** <sub>$i,j$</sub> ,  $\forall (i, j) \in \mathcal{M} \times \mathcal{N}$ , in Subsection III-B) and  $M$  subproblems (referring to **P3** <sub>$i$</sub> ,  $\forall i \in \mathcal{M}$ , in Subsection III-C), respectively. Among them, each **P2** <sub>$i,j$</sub>  corresponds to the

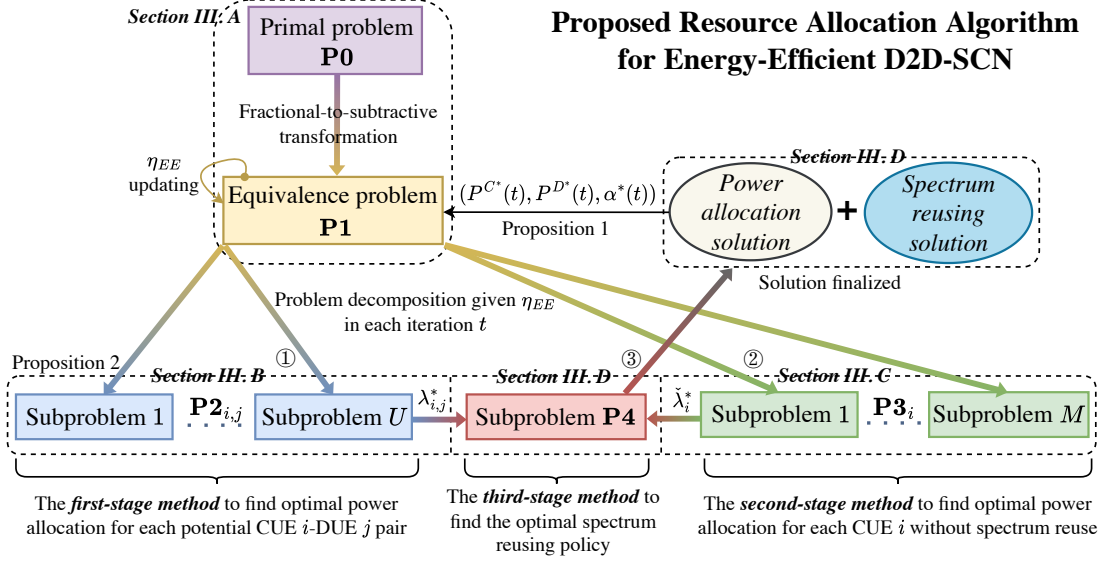


Fig. 2. Illustration of the proposed resource allocation algorithm.

power allocation problem for a potential spectrum reusing pair of CUE  $i$  and DUE  $j$ , while each  $\mathbf{P3}_i$  corresponds to that for each CUE  $i$  without spectrum reusing. After solving all these subproblems, the spectrum reusing policy w.r.t.  $\alpha$  is optimally finalized (referring to  $\mathbf{P4}$  in Subsection III-D). In the end, we present the workflow of our proposed solution along with its complexity analysis in Subsection III-E.

#### A. Fractional-to-Subtractive Problem Transformation

Since the objective  $\eta_{EE}$  in the primal problem  $\mathbf{P0}$  is quite complicated and hard to deal, we first employ the Dinkelbach's method [28] to transform  $\eta_{EE}$  into a subtractive-form function  $F(\eta_{EE})$  to make it decomposable and tractable. The transformation is established given in the following proposition.

**Proposition 1.**  $\mathbf{P0}$  must have the same optimal solution as

$$\mathbf{P1}: F(\eta_{EE}) = \max_{\mathbf{P}^C, \mathbf{P}^D, \alpha} V^{total} - \eta_{EE} \cdot E^{total} \quad (9)$$

$$\text{s.t.} \quad (8a) - (8g), \quad (9a)$$

if and only if  $F(\eta_{EE}) = 0$ .

*Proof:* Please see Appendix A. ■

From Proposition 1, our optimization goal is to solve  $\mathbf{P1}$  given any  $\eta_{EE}$  while requiring the iterative update for  $\eta_{EE}$  such that  $F(\eta_{EE})$  eventually approaches 0, and thus reaching the optimality of  $\mathbf{P0}$ . Specifically, we begin by assigning an arbitrary non-negative initial value to  $\eta_{EE}$  for  $\mathbf{P1}$ , which needs to be updated in each iteration according to the following rule:

$$\eta_{EE}(t+1) = \frac{V^{total}(\mathbf{P}^{C^*}(t), \mathbf{P}^{D^*}(t), \alpha^*(t))}{E^{total}(\mathbf{P}^{C^*}(t), \mathbf{P}^{D^*}(t), \alpha^*(t))}, \quad (10)$$

where  $(\mathbf{P}^{C^*}(t), \mathbf{P}^{D^*}(t), \alpha^*(t))$  is the optimal solution to  $\mathbf{P1}$  in iteration  $t$ .  $V^{total}(\cdot)$  and  $E^{total}(\cdot)$  represent the functional forms of  $V^{total}$  and  $E^{total}$  w.r.t. the variables  $(\mathbf{P}^C, \mathbf{P}^D, \alpha)$ , respectively. Note that such iterative update should be stopped when either reaching the maximum number of iterations

## Proposed Resource Allocation Algorithm for Energy-Efficient D2D-SCN

(denoted by  $Q$ ) or satisfying a condition of  $F(\eta_{EE}(t)) < \epsilon$ , where  $\epsilon$  is a preset small positive value [24]. Most importantly, it has been proved that if  $Q$  is large enough, the convergence of  $\eta_{EE}$  can be guaranteed such that the optimality condition in Proposition 1 is satisfied, i.e.,  $F(\eta_{EE}(t)) = 0$ , and the details of proof can refer to [25] and [28].

Given any  $\eta_{EE}$  in each iteration, we now concentrate upon how to reach the optimality of  $\mathbf{P1}$ . However, solving such a problem is still tricky due to the mixed integer variables in its highly complex objective function (9). To this end,  $\mathbf{P1}$  will be first decomposed into multiple subproblems, and then we specially propose a three-stage method to separately obtain the optimal power allocation scheme  $(\mathbf{P}^C, \mathbf{P}^D)$  and the optimal spectrum reusing policy  $\alpha$  with polynomial-time complexity.

#### B. Optimal Power Allocation for A Single CUE-DUE Pair

In the first stage, the power allocation scheme is optimized for a specific pair of CUE  $i$  ( $\forall i \in \mathcal{M}$ ) and DUE  $j$  ( $\forall j \in \mathcal{N}$ ). As such, we construct  $U = M \times N$  subproblems, each of which is denoted as  $\mathbf{P2}_{i,j}$  and the objective is to maximize energy efficiency for the single spectrum reusing pair. It is worth pointing out that combining the optimal single-pair solutions to these  $\mathbf{P2}_{i,j}$  cannot directly achieve the optimal power allocation strategy for  $\mathbf{P1}$ , but these solutions will be used to construct the subsequent spectrum reuse subproblem so as to help finalize the optimal strategy for  $\mathbf{P1}$ . Accordingly, when DUE  $j$  reuses the subchannel of CUE  $i$  (i.e.,  $\alpha_{i,j} = 1$ ), given any  $\eta_{EE}$ ,  $\mathbf{P2}_{i,j}$  becomes

$$\mathbf{P2}_{i,j}: \max_{P_i^C, P_j^D} \lambda_{i,j} \quad (11)$$

$$\text{s.t.} \quad V_i^C \geq V_{min}^C, \quad (11a)$$

$$V_j^D \geq V_{min}^D, \quad (11b)$$

$$0 \leq P_i^C \leq P_{max}^C, \quad (11c)$$

$$0 \leq P_j^D \leq P_{max}^D. \quad (11d)$$

In particular,  $\lambda_{i,j}$  is defined as the sum of all the terms related to the fixed pair of CUE  $i$  and DUE  $j$  in  $F(\eta_{EE})$ , given by (12) at the bottom of the next page, in which  $\sigma_i^C$  and  $\sigma_j^D$  are defined for brevity. In addition,  $r_i^C$  and  $r_j^D$  expressed in (12) are calculated by substituting  $\alpha_{i,j} = 1$  into (1) and (2), respectively, which can be found as

$$\overline{r_i^C} = W \log_2 \left( 1 + \frac{P_i^C G_{i,B}}{\delta^2 + P_j^D G_{j,B}} \right) \quad (13)$$

and

$$\overline{r_j^D} = W \log_2 \left( 1 + \frac{P_j^D G_j^D}{\delta^2 + P_i^C G_{i,j}} \right). \quad (14)$$

Notice that  $\theta_i^C$  and  $\theta_j^D$  are two positive parameters as in (3) and (4), and thus constraints (11a) and (11b) in  $\mathbf{P2}_{i,j}$  can be smoothly transformed to  $\overline{r_i^C} \geq L \lceil V_{min}^C / \theta_i^C \rceil$  and  $\overline{r_j^D} \geq L \lceil V_{min}^D / \theta_j^D \rceil$ , respectively. By further considering the boundary case of either of the two constraints, according to (13) and (14),  $P_j^D$  can clearly be expressed as a linear function of  $P_i^C$ . On this basis, Fig. 3 depicts three possible cases for the closed feasible region  $\psi$  w.r.t.  $(P_i^C, P_j^D)$ . Now, if we first generate an arbitrary feasible solution in  $\psi$ , denoted as  $(\widetilde{P_i^C}, \widetilde{P_j^D})$ , then considering a special case of substituting  $(\widetilde{P_i^C}, \widetilde{P_j^D})$  into the first term  $\sigma_i^C \lceil \overline{r_i^C} / L \rceil$  in (12), such that

$$\sigma_i^C \left[ \frac{W}{L} \log_2 \left( 1 + \frac{\widetilde{P_i^C} G_{i,B}}{\delta^2 + \widetilde{P_j^D} G_{j,B}} \right) \right] \triangleq \lambda_0, \quad (15)$$

where  $\lambda_0$  is denoted as the corresponding solved value. Based on (15), there must be a line segment w.r.t.  $(P_i^C, P_j^D) \in \psi$  passing through the point  $(\widetilde{P_i^C}, \widetilde{P_j^D})$ , which can be expressed as a linear equation of  $P_i^C$  w.r.t.  $P_j^D$ , i.e.,

$$P_i^C = \frac{G_{j,B} \left( 2^{\frac{L}{W} \lceil \lambda_0 / \sigma_i^C \rceil} - 1 \right)}{G_{i,B}} P_j^D + \frac{\delta^2 \left( 2^{\frac{L}{W} \lceil \lambda_0 / \sigma_i^C \rceil} - 1 \right)}{G_{i,B}} \triangleq k_0 P_j^D + b_0, \quad (16)$$

where  $k_0$  and  $b_0$  are denoted as constants. Clearly, any point  $(P_i^C, P_j^D)$  on (16) results in the term  $\sigma_i^C \lceil \overline{r_i^C} / L \rceil$  being computed as  $\lambda_0$ . Keeping this in mind, we then concentrate

upon the remaining terms of  $\lambda_{i,j}$ . By employing (16), we can substitute  $P_i^C$  in (12) by  $P_j^D$ , such that

$$\begin{aligned} \lambda_{i,j} &= \sigma_j^D \left[ \overline{r_j^D} / L \right] - \eta_{EE} \xi (P_i^C + P_j^D) + \lambda_0 \\ &= \sigma_j^D \left[ \frac{W}{L} \log_2 \left( 1 + \frac{G_j^D}{[(\delta^2 + G_{i,j} b_0) / P_j^D] + G_{i,j} k_0} \right) \right] \\ &\quad - \eta_{EE} \xi [(k_0 + 1) P_j^D + b_0] + \lambda_0 \\ &\triangleq \sigma_j^D [\phi_1(P_j^D)] + \phi_2(P_j^D) + \lambda_0 \\ &\triangleq \widetilde{\lambda}_1(P_j^D) + \lambda_0. \end{aligned} \quad (17)$$

Here,  $\phi_1(P_j^D)$  is the logarithmic function of  $P_j^D$ ,  $\phi_2(P_j^D)$  is the linear function of  $P_j^D$ , and  $\widetilde{\lambda}_1(P_j^D)$  is the combinatorial function of  $\phi_1(P_j^D)$  and  $\phi_2(P_j^D)$ .

Notice that  $\phi_1(P_j^D)$  is increasing w.r.t.  $P_j^D$ , and hence  $\sigma_j^D [\phi_1(P_j^D)]$  clearly becomes a monotone staircase function of  $P_j^D$ , and its monotonicity depends on the positivity or negativity of  $\sigma_j^D$ . Combined with the linear property of  $\phi_2(P_j^D)$ , it is easily found that the optimal  $P_j^D$  leading to the maximal  $\lambda_{i,j}$  must be exactly one endpoint of a particular staircase of  $\sigma_j^D [\phi_1(P_j^D)]$ . For instance, if  $\sigma_j^D \geq 0$  and  $-\eta_{EE} \xi (k_0 + 1) \geq 0$ , the optimal  $P_j^D$  must be the rightmost endpoint of the rightmost staircase of  $\sigma_j^D [\phi_1(P_j^D)]$ . Moreover, considering the closed feasible region  $\psi$ , the number of staircases of  $\sigma_j^D [\phi_1(P_j^D)]$  must be limited, thereby a brute-force search can be applied to determine the optimal  $P_j^D$ . Afterward, the optimal  $P_i^C$  should be obtained based on (16). In summary, over the set of points on the line segment obtained by fixing the first term in (12), we can always find the optimal  $(P_i^C, P_j^D)$  to maximize  $\lambda_{i,j}$ .

Next, if we substitute the same solution  $(\widetilde{P_i^C}, \widetilde{P_j^D})$  into the second term  $\sigma_j^D \lceil \overline{r_j^D} / L \rceil$  in (12), another line segment can be determined similar to the rationale behind (15). Different with (16), this line segment is expressed as a linear equation of  $P_j^D$  w.r.t.  $P_i^C$ . Given that, substituting  $P_j^D$  in (12) by  $P_i^C$  can yield an expression form of  $\lambda_{i,j}$  w.r.t.  $P_i^C$ , denoted by  $\lambda_{i,j} \triangleq \widetilde{\lambda}_2(P_i^C) + \lambda'_0$ . Likewise,  $\widetilde{\lambda}_2(P_i^C)$  is the combinatorial function of one staircase function and one linear function w.r.t.  $P_i^C$ . By again leveraging the brute-force search, we can also find the optimal  $(P_i^C, P_j^D)$  over the set of points on the line segment obtained by fixing the second term in (12).

In view of the above, the following proposition shows how  $\widetilde{\lambda}_1(P_j^D)$  and  $\widetilde{\lambda}_2(P_i^C)$  influence the optimality of  $\mathbf{P2}_{i,j}$ .

$$\begin{aligned} \lambda_{i,j} &= \theta_i^C \left[ \frac{\overline{r_i^C}}{L} \right] + \theta_j^D \left[ \frac{\overline{r_j^D}}{L} \right] - \eta_{EE} \left[ P^{enc} \left( \left[ \frac{\overline{r_i^C}}{L} \right] + \left[ \frac{\overline{r_j^D}}{L} \right] \right) + \xi (P_i^C + P_j^D) \right] \\ &= (\theta_i^C - \eta_{EE} P^{enc}) \left[ \frac{\overline{r_i^C}}{L} \right] + (\theta_j^D - \eta_{EE} P^{enc}) \left[ \frac{\overline{r_j^D}}{L} \right] - \eta_{EE} \xi (P_i^C + P_j^D) \\ &\triangleq \sigma_i^C \left[ \frac{\overline{r_i^C}}{L} \right] + \sigma_j^D \left[ \frac{\overline{r_j^D}}{L} \right] - \eta_{EE} \xi (P_i^C + P_j^D). \end{aligned} \quad (12)$$

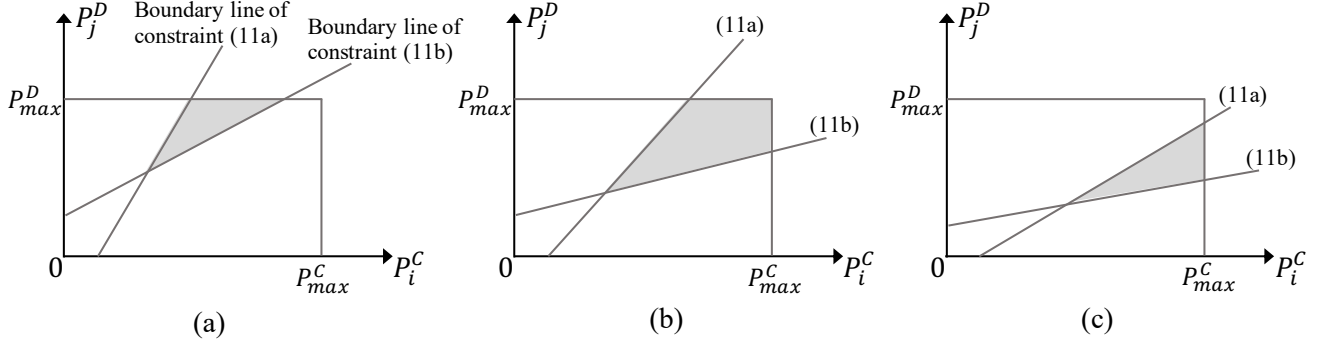


Fig. 3. Three possible cases of the feasible power allocation region  $\psi$  for each pair of CUE  $i$  and DUE  $j$  w.r.t.  $\mathbf{P2}_{i,j}$ .

**Proposition 2.** Given any feasible solution  $(\overleftarrow{P}_i^C, \overleftarrow{P}_j^D) \in \psi$  of  $\mathbf{P2}_{i,j}$ , let  $(\overleftarrow{P}_i^C, \overleftarrow{P}_j^D)$  be the optimal point on the line segment w.r.t.  $\tilde{\lambda}_1(P_j^D)$ , and let  $(\overrightarrow{P}_i^C, \overrightarrow{P}_j^D)$  be the optimal point at the line segment w.r.t.  $\tilde{\lambda}_2(P_i^C)$ . If we consider the optimal solution to  $\mathbf{P2}_{i,j}$  denoted as  $(P_i^{C*}, P_j^{D*})$ , it must satisfy

$$(P_i^{C*}, P_j^{D*}) \in \left\{ \left( \overleftarrow{P}_i^C, \overleftarrow{P}_j^D \right) \mid \left( \overleftarrow{P}_i^C, \overleftarrow{P}_j^D \right) = \left( \overrightarrow{P}_i^C, \overrightarrow{P}_j^D \right) \in \psi \right\}. \quad (18)$$

*Proof:* Please see Appendix B. ■

From Proposition 2, it is seen that  $\mathbf{P2}_{i,j}$ 's optimal solution  $(P_i^{C*}, P_j^{D*})$  must be the coincide point that makes  $\tilde{\lambda}_1(P_j^D)$  and  $\tilde{\lambda}_2(P_i^C)$  reach their respective maxima at the same time. In line with this, we specially devise a heuristic search algorithm to efficiently determine the optimal power allocation strategy for each possible CUE-DUE pair. In detail, our power allocation solution is realized by the following five phases:

- (1) *Initial Feasible Solution Generation:* According to the feasible region  $\psi$  determined by all constraints of  $\mathbf{P2}_{i,j}$ , we need to first generate an initial feasible solution  $(\overleftarrow{P}_i^C, \overleftarrow{P}_j^D)$  as the search starting point. For simplicity,  $(\overleftarrow{P}_i^C, \overleftarrow{P}_j^D)$  can be set as one of the corners of  $\psi$  in Fig. 3.
- (2) *Optimal Line Point Search for Maximum  $\tilde{\lambda}_1(P_j^D)$ :* By executing the procedures in (15)-(17), the close-form expression of  $\tilde{\lambda}_1(P_j^D)$  is obtained. Note that the domain of  $P_j^D$  should be constrained by the line segment as in (16). On this basis, by directly substituting the minimum and maximum  $P_j^D$  into  $\sigma_j^D[\phi_1(P_j^D)]$ , respectively, the values and the two endpoints of all staircases can be obtained, to which the brute-force search is applied to determine  $(\overleftarrow{P}_i^C, \overleftarrow{P}_j^D)$  and it is not difficult to solve.
- (3) *Optimal Line Point Search for Maximum  $\tilde{\lambda}_2(P_i^C)$ :* We substitute the obtained  $(\overleftarrow{P}_i^C, \overleftarrow{P}_j^D)$  into the second term  $\sigma_j^D[r_j^D/L]$  in (12) to obtain the close-form expressions of its corresponding line segment and  $\tilde{\lambda}_2(P_i^C)$ . By substituting the minimum and maximum  $P_i^C$  and again leveraging the brute-force search,  $(\overrightarrow{P}_i^C, \overrightarrow{P}_j^D)$  is obtained.
- (4) *Searching Termination Check:* If  $(\overleftarrow{P}_i^C, \overleftarrow{P}_j^D) =$

$(\overrightarrow{P}_i^C, \overrightarrow{P}_j^D)$ , i.e., the optimal point of the previous line segment is also optimal for the current searching line segment, this round of search is terminated. Otherwise, the obtained  $(\overleftarrow{P}_i^C, \overleftarrow{P}_j^D)$  is substituted into the first term  $\sigma_i^C[r_i^C/L]$  in (12), and then keep repeating Phases (2) and (3) until  $(\overleftarrow{P}_i^C, \overleftarrow{P}_j^D) = (\overrightarrow{P}_i^C, \overrightarrow{P}_j^D)$  is satisfied. After the coincide point is obtained, according to Proposition 2, this point may fall into a local optimum of  $\mathbf{P2}_{i,j}$ , and hence we add it into a list, denoted by  $\mathcal{I} = \left\{ \left( \overleftarrow{P}_i^C, \overleftarrow{P}_j^D \right) \mid \left( \overleftarrow{P}_i^C, \overleftarrow{P}_j^D \right) = \left( \overrightarrow{P}_i^C, \overrightarrow{P}_j^D \right) \in \psi \right\}$ , for record.

- (5) *Multiple Rounds of Searches:* To prevent the algorithm trapping into the local optimum, we set Phases (1)-(4) as one round of the search. Then, multiple rounds of search are repeated until reaching a preset maximum round restriction, and in different rounds, the initial feasible solution  $(\overleftarrow{P}_i^C, \overleftarrow{P}_j^D)$  should always be different. Consequently, the optimal power allocation strategy  $(P_i^{C*}, P_j^{D*})$  is finalized by comparing all the solutions recorded in  $\mathcal{I}$ .

### C. Power Allocation for each CUE Without Spectrum Sharing

Since the preset number of DUEs does not exceed that of CUEs (i.e.,  $N \leq M$ ), there must be a part of CUEs' sub-channels not reused by any DUE. Accordingly, it is also necessary to determine the optimal power allocation solution for each CUE  $i$  without spectrum sharing, and thus our second-stage problem  $\mathbf{P3}_i$  ( $\forall i \in \mathcal{M}$ ) becomes

$$\mathbf{P3}_i : \max_{P_i^C} \tilde{\lambda}_i \quad (19)$$

$$\text{s.t. } \theta_i^C [r_i^C/L] \geq V_{min}^C, \quad (19a)$$

$$(11c), \quad (19b)$$

where  $r_i^C = W \log_2 \left( 1 + \frac{P_i^C G_{i,B}}{\delta^2} \right)$ , representing the achievable bit rate at CUE  $i$  when  $\alpha_{i,j} = 0$ , and  $\tilde{\lambda}_i = \sigma_i^C [r_i^C/L] - \eta_{EE} \xi P_i^C$ , indicating all the terms related to only CUE  $i$  in (9).

Combined constraint (19a) with (19b), the domain of feasible  $P_i^C$  is confined as  $[\delta^2 (2^{\frac{1}{W}} [V_{min}^C / \theta_i^C] - 1) / G_{i,B}] \leq P_i^C \leq P_{max}^C$ . With this, it is further observed that the first term  $\sigma_i^C [r_i^C/L]$  in  $\tilde{\lambda}_i$  is a monotone staircase function of  $P_i^C$ ,

while its second term  $-\eta_{EE}\xi P_i^C$  is a linear function of  $P_i^C$ . Recap our previous analysis to (17), the optimal  $P_i^C$  to each  $\mathbf{P3}_i$  can be straightforwardly obtained by again employing the brute-force search with acceptable computation complexity.

#### D. Optimal Spectrum Reusing Policy

Given any  $\eta_{EE}$  in each iteration of  $\mathbf{P1}$ , our third-stage method is to finalized the optimal spectrum reusing policy for all CUEs and DUEs, based on the obtained power allocation solutions to both  $\mathbf{P2}_{i,j}$  and  $\mathbf{P3}_i$ . First let  $\lambda_{i,j}^*$  denote the maximum  $\lambda_{i,j}$  at each potential spectrum reusing pair of CUE  $i$  and DUE  $j$  by solving each  $\mathbf{P2}_{i,j}$ , and let  $\check{\lambda}_i^*$  denote the maximum  $\check{\lambda}_i$  at the single CUE  $i$  by solving each  $\mathbf{P3}_i$ . As such, the spectrum reusing problem becomes a variant of the weighted bipartite matching optimization problem, i.e.,

$$\begin{aligned} \mathbf{P4}: \max_{\alpha} \quad & \sum_{i \in \mathcal{M}} \sum_{j \in \mathcal{N}} \alpha_{i,j} \lambda_{i,j}^* + \sum_{i \in \mathcal{M}} \check{\lambda}_i^* \left( 1 - \sum_{j \in \mathcal{N}} \alpha_{i,j} \right) \\ \text{s.t.} \quad & \text{(8e) - (8g)}. \end{aligned} \quad (20)$$

(20a)

Clearly,  $\mathbf{P4}$  is an  $M$ -to- $N$  bipartite matching problem, which should be first expanded into an  $M$ -to- $M$  case for tractability as  $M \geq N$ . Specifically, let  $\Omega$  denote an  $M \times M$  matrix, where all rows represent  $M$  CUEs and the first  $N$  columns represent all DUEs. Besides, the elements in the first  $N$  columns of  $\Omega$  are filled with all  $\lambda_{i,j}^*$ , and the elements in each of the remaining  $M - N$  columns are filled with the same  $\check{\lambda}_i^*$ . As such,  $\Omega$  is found by

$$\Omega = \begin{array}{c} \begin{array}{cc} \text{Representing } N \text{ DUEs in } \mathcal{N} & \text{Expanded } (M-N) \text{ columns} \end{array} \\ \left[ \begin{array}{cccc|ccc} \lambda_{1,1}^* & \lambda_{1,2}^* & \cdots & \lambda_{1,N}^* & \check{\lambda}_1^* & \cdots & \check{\lambda}_1^* \\ \lambda_{2,1}^* & \lambda_{2,2}^* & \cdots & \lambda_{2,N}^* & \check{\lambda}_2^* & \cdots & \check{\lambda}_2^* \\ \vdots & \vdots & \ddots & \vdots & \vdots & \ddots & \vdots \\ \lambda_{M,1}^* & \lambda_{M,2}^* & \cdots & \lambda_{M,N}^* & \check{\lambda}_M^* & \cdots & \check{\lambda}_M^* \end{array} \right] \end{array}. \quad (21)$$

Correspondingly, a new variable set needs to be defined as  $\alpha' = \{\alpha_{i,j'} \mid i \in \mathcal{M}, j' \in \mathcal{M}\}$ , and then  $\mathbf{P4}$  can be converted into an  $M$ -to- $M$  bipartite matching problem as

$$\mathbf{P4.1}: \max_{\alpha'} \quad \Omega \odot \alpha' \quad (22)$$

$$\text{s.t.} \quad \sum_{j' \in \mathcal{M}} \alpha_{i,j'} = 1, \quad \forall i \in \mathcal{M}, \quad (22a)$$

$$\sum_{i \in \mathcal{M}} \alpha_{i,j'} = 1, \quad \forall j' \in \mathcal{M}, \quad (22b)$$

$$\alpha_{i,j'} \in \{0, 1\}, \quad \forall (i, j') \in \mathcal{M} \times \mathcal{M}, \quad (22c)$$

where the operator  $\odot$  represents the Hadamard product. For such a standard assignment problem,  $\mathbf{P4.1}$  can be efficiently solved in polynomial time by applying the Hungarian method [29]. After obtaining each optimal  $\alpha_{i,j'}$  (denoted as  $\alpha_{i,j'}^*$ ), it is easily derived that each DUE  $j$  can reuse the

spectrum of its optimal CUE  $i$  (denoted by  $\alpha_{i,j}^*$ ) if and only if it satisfies the following condition

$$\alpha_{i,j}^* = \begin{cases} 1, & \text{if } \alpha_{i,j'}^* = 1 \text{ and } j' \in \mathcal{N} = \{1, 2, \dots, N\}; \\ 0, & \text{otherwise.} \end{cases} \quad (23)$$

In this way, given any  $\eta_{EE}$  in each iteration w.r.t.  $\mathbf{P1}$ , the optimal spectrum reusing scheme is now finalized along with the optimal power allocation policy at each CUE and DUE.

#### E. Algorithm Analysis

To better demonstrate the full procedure of the proposed solution shown in Fig. 2, we summarize the technical points and enclose them in Algorithm 1.

##### Algorithm 1 Proposed Resource Allocation for D2D-SCN

**Input:** The network parameters  $M, N, K, W, L, \delta^2, P^{enc}, \xi, P_{max}^C, P_{max}^D, V_{min}^C, V_{min}^D$ , and each SemCom user's parameters  $G_{i,B}, G_{j,B}, G_j^D, G_{i,j}, u_{i,k}^C, u_{j,k}^D, \beta_i^C, \beta_j^D$

**Output:** The optimal power allocation policy ( $\mathbf{P}^{C*}, \mathbf{P}^{D*}$ ) and the optimal spectrum reusing strategy  $\alpha^*$

- 1: Initialize iteration index  $t \leftarrow 1$  and  $\eta_{EE}(1) \leftarrow 0$  for  $\mathbf{P1}$
- 2: Set  $Q$  (large) and  $\epsilon$  (small) to proper positive values
- 3: **while**  $t \leq Q$  **do**
- 4:   **for**  $i \leftarrow 1$  to  $M$  **do**
- 5:     **for**  $j \leftarrow 1$  to  $N$  **do**
- 6:       Initialize the search round index as  $\tilde{t} \leftarrow 1$  and the
- 7:       solution list  $\mathcal{I}(1) \leftarrow \emptyset$  for solving each  $\mathbf{P2}_{i,j}$ .
- 8:       Set the maximum number of search rounds as  $\tilde{Q}$
- 9:       **while**  $\tilde{t} \leq \tilde{Q}$  **do**
- 10:          Choose an arbitrary point in  $\psi$  as  $(\overleftarrow{P}_i^C, \overleftarrow{P}_j^D)$
- 11:          Find  $(\overleftarrow{P}_i^C, \overleftarrow{P}_j^D)$  w.r.t.  $(\overleftarrow{P}_i^C, \overleftarrow{P}_j^D)$  by Phase (2)
- 12:          Find  $(\overrightarrow{P}_i^C, \overrightarrow{P}_j^D)$  w.r.t.  $(\overleftarrow{P}_i^C, \overleftarrow{P}_j^D)$  by Phase (3)
- 13:          **while**  $(\overleftarrow{P}_i^C, \overleftarrow{P}_j^D) \neq (\overrightarrow{P}_i^C, \overrightarrow{P}_j^D)$  **do**
- 14:            $(\overleftarrow{P}_i^C, \overleftarrow{P}_j^D) \leftarrow (\overrightarrow{P}_i^C, \overrightarrow{P}_j^D)$
- 15:           **repeat** Lines 11 and 12
- 16:          **end while**
- 17:           $\mathcal{I}(\tilde{t} + 1) \leftarrow \mathcal{I}(\tilde{t}) \cup \{(\overleftarrow{P}_i^C, \overleftarrow{P}_j^D)\}$
- 18:           $\tilde{t} \leftarrow \tilde{t} + 1$
- 19:       **end while**
- 20:       Finalize  $(P_i^{C*}, P_j^{D*})$  for each potential CUE  $i$ -
- 21:       DUE  $j$  pair by comparing all solutions in  $\mathcal{I}(\tilde{Q})$
- 22:       Compute  $\lambda_{i,j}^*(t)$  by (11) for  $\mathbf{P4}$
- 23:     **end for**
- 24:   **end for**
- 25:   **for**  $i \leftarrow 1$  to  $M$  **do**
- 26:     Finalize the optimal  $P_i^C$  for each single CUE  $i$  by
- 27:     employing the brute-force search to solve  $\mathbf{P3}_i$
- 28:     Compute  $\check{\lambda}_i^*(t)$  by (19) for  $\mathbf{P4}$
- 29:   **end for**
- 30:   Generate  $\Omega$  according to (21)
- 31:   Solve  $\mathbf{P4.1}$  by using the Hungarian method



```

32: Determine each  $\alpha_{i,j}^*(t)$  by (23)
33: Finalize  $\mathbf{P}^{C^*}(t)$ ,  $\mathbf{P}^{D^*}(t)$ , and  $\alpha^*(t)$  by backtracking
34: through the element corresponding to  $\alpha_{i,j}^*(t)$  in  $\Omega$ 
35: Calculate  $F(\eta_{EE}(t))$  by substituting the finalized
36:  $\mathbf{P}^{C^*}(t)$ ,  $\mathbf{P}^{D^*}(t)$ , and  $\alpha^*(t)$  into (9)
37: if  $F(\eta_{EE}(t)) < \epsilon$  then
38: return  $(\mathbf{P}^{C^*}, \mathbf{P}^{D^*}, \alpha^*) \leftarrow (\mathbf{P}^{C^*}(t), \mathbf{P}^{D^*}(t), \alpha^*(t))$ 

39: break
40: else
41: Update  $\eta_{EE}(t+1)$  by (10)
42:  $t \leftarrow t+1$ 
43: end if
44: end while
45: return  $(\mathbf{P}^{C^*}, \mathbf{P}^{D^*}, \alpha^*) \leftarrow (\mathbf{P}^{C^*}(Q), \mathbf{P}^{D^*}(Q), \alpha^*(Q))$ 

```

Regarding the computational complexity of Algorithm 1, it is first seen that in each search round for solving each  $\mathbf{P2}_{i,j}$ , it takes several iterations (Lines 11-16) to determine one viable solution in  $\mathcal{I}$ , and in each iteration, the brute-force search needs to be executed once to obtain  $(\overrightarrow{P_i^C}, \overrightarrow{P_j^D})$  or  $(\overrightarrow{P_i^D}, \overrightarrow{P_j^C})$ . Hence, if denoting the maximum number of iterations w.r.t. Lines 11-16 as  $H$  and the maximum number of staircase w.r.t. each brute-force search as  $\tilde{H}$ , then solving each  $\mathbf{P2}_{i,j}$  would have the complexity of  $\mathcal{O}(\tilde{Q}H\tilde{H})$ . Likewise, solving each  $\mathbf{P3}_i$  has the complexity of  $\mathcal{O}(\tilde{H})$ . Moreover, since the  $M$ -to- $M$  bipartite matching problem w.r.t.  $\mathbf{P4.1}$  can be solved by the Hungarian method with the complexity of  $\mathcal{O}(M^3)$  [30], the complexity for solving  $\mathbf{P4}$  is  $\mathcal{O}(M^3)$ . Accordingly, the proposed Algorithm 1 has a polynomial-time overall complexity of  $\mathcal{O}(QM\tilde{N}\tilde{Q}H\tilde{H} + M^3)$ .

#### IV. NUMERICAL RESULTS AND DISCUSSIONS

In this section, numerical evaluations are conducted to demonstrate the performance of our proposed power allocation and spectrum reusing solutions in the D2D-SCN, where we employ Python 3.7-based PyCharm as the simulator platform and implement it in a workstation PC featuring the AMD Ryzen-9-7900X processor with 12 CPU cores and 128 GB RAM. In the basic system setup, we first model a single-cell circular area with a radius of 300 meters, in which multiple CUEs and DUEs are randomly dropped, and the distance between the transceiver of each DUE is randomly generated between 50 and 200 meters. For the energy efficiency model, each SemCom device is assumed to have a fixed power amplifier efficiency of 35 percent [31], i.e.,  $\xi = 1/0.35 = 2.8571$ , and let the circuit power consumption required for encoding one semantic triplet  $P^{enc} = 0.5$  mW [26]. For brevity, other simulation parameters along with their values are summarized in Table I. For the simulated SemCom model, we set  $K = 20$  as the total number of wireless SemCom services in the D2D-SCN. Besides, the preference ranking of each CUE (i.e.,  $u_{i,k}^C$ ) and DUE (i.e.,  $u_{j,k}^D$ ) for all these services is generated in an independent and random manner, while the skewness of the Zipf distribution at each CUE (i.e.,  $\beta_i^C$ ) and DUE (i.e.,  $\beta_j^D$ ) is randomly distributed in a range of  $0.5 \sim 1.5$  [19]. As for the solution settings, the maximum number of iterations for

TABLE I  
SIMULATION PARAMETERS

Parameters	Values
Number of SemCom-enabled CUEs ( $M$ )	50
Number of SemCom-enabled DUEs ( $N$ )	30
Subchannel bandwidth ( $W$ )	$10/M$ MHz
Maximum transmit power of each CUE ( $P_{max}^C$ )	23 dBm [32]
Maximum transmit power of each DUE ( $P_{max}^D$ )	21 dBm [32]
Noise power ( $\delta^2$ )	-111.45 dBm
Path loss model for cellular links	$128.1 + 37.6 \log_{10}(d \text{ [km]})$ dB
Path loss model for D2D links	$148 + 40 \log_{10}(d \text{ [km]})$ dB [33]
Average number of bits required for encoding one semantic triplet ( $L$ )	50 bits [19]

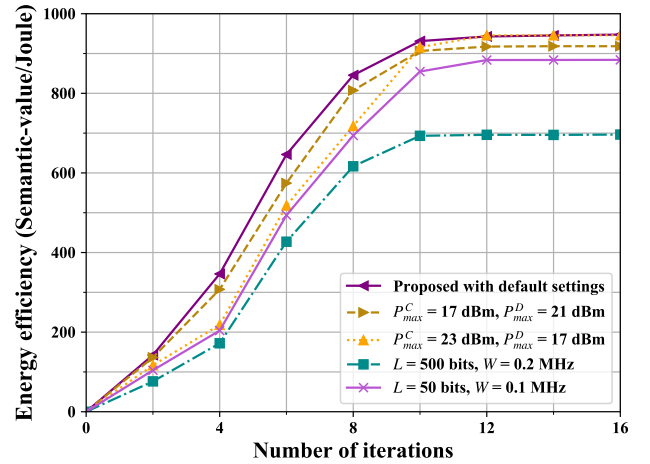


Fig. 4. Energy efficiency ( $\eta_{EE}$ ) versus different numbers of iterations.

updating  $\eta_{EE}$  in  $\mathbf{P1}$  is set as  $Q = 20$ , and its convergence threshold  $\epsilon$  is 0.01. In addition, the minimum semantic value threshold is set as the same for all CUEs and DUEs, i.e.,  $V_{min} = V_{min}^C = V_{min}^D = 50$ . It is worth mentioning that all the above parameter values are set by default unless otherwise specified, and all subsequent numerical results are obtained by averaging over a sufficiently large number of trials.

For comparison purposes, here we employ two resource allocation benchmarks in D2D-SCNs: (I) Maximum power allocation plus random spectrum reusing [34], which means that each user is allocated with its maximum allowable transmit power while each DUE randomly reuses the subchannel of one CUE; (II) Random power allocation [35] plus distance-based spectrum reusing [36], where each user is allocated with the randomized transmit power while each DUE reuses the subchannel of the CUE furthest away from itself to reduce the interference impact as much as possible.

As presented in Fig. 4, we first investigate the convergence and analyze the energy efficiency performance (i.e.,  $\eta_{EE}$ ) of the proposed solution, where different settings of  $P_{max}^C = 17$

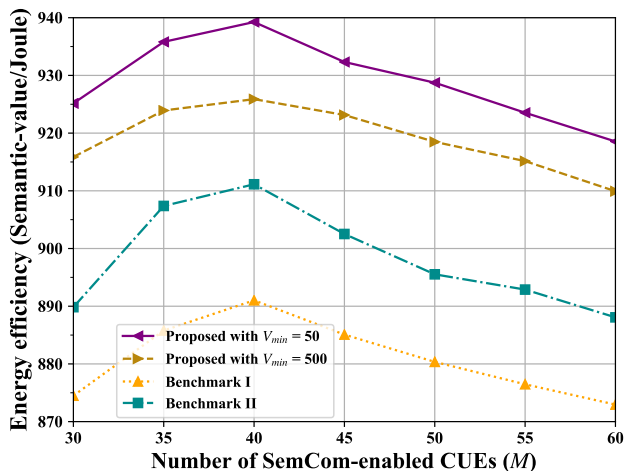


Fig. 5. Energy efficiency versus different numbers of CUEs.

dBm,  $P_{max}^D = 17$  dBm,  $L = 500$  bits, and  $W = 0.1$  MHz are used in comparison with those in Table I. With the increase of iterations, it can be observed that the proposed solution in different settings can always converge to their respective maximum  $\eta_{EE}$  while having the same convergence speed, i.e., they all reach convergence after around 12 iterations. This phenomenon indicates that our designed algorithm is not affected by changes of system parameter values and is therefore very ideal for practical implementation. Meanwhile, compared with the default settings, Fig. 4 further shows that the worse  $\eta_{EE}$  occurs at the smaller  $P_{max}^C$  and  $W$  as well as the larger  $L$ . The underlying reason is that the stronger limitation on CUEs' maximum transmit power leads to a certain degree of semantic value degradation especially for those CUEs without spectrum sharing, as they tend to use the maximum  $P_{max}^C$  compared with these with spectrum sharing. Besides, both the smaller  $W$  and the larger  $L$  can result in the lower achievable rate of semantic triplet transmission per link, which justifies the reduction in the energy efficiency.

Fig. 5 shows the objective performance metric of  $\eta_{EE}$  obtained under varying numbers of CUEs (i.e.,  $M$ ) between 30 and 60, where two different semantic value thresholds of  $V_{min} = 50$  and  $V_{min} = 500$  are considered. Compared with the two benchmarks, it is seen that our proposed solution always guarantees a significant performance gain with the changes of  $M$ . For instance, when  $M = 35$ , the energy efficiency of 935.8 semantic-value/Joule is observed by the proposed solution at  $V_{min} = 50$ , which increases 5.76% performance compared to Benchmark I and 3.2% compared to Benchmark II. Moreover, as  $M$  increases, the energy efficiency of the proposed solution rises at the beginning from 30 to 40, and then drops gradually. This is because the increase of  $M$  at the beginning can provide each DUE more options to choose a better CUE for spectrum reusing and thus leading to a better energy efficiency performance. Then, as  $M$  keeps growing, the subchannel bandwidth  $W$  averaged to each CUE becomes fewer due to the fixed total system bandwidth, but the number of DUEs remains constant in Fig. 5. Hence, after the point of  $M = 40$ , the reduction in energy efficiency due

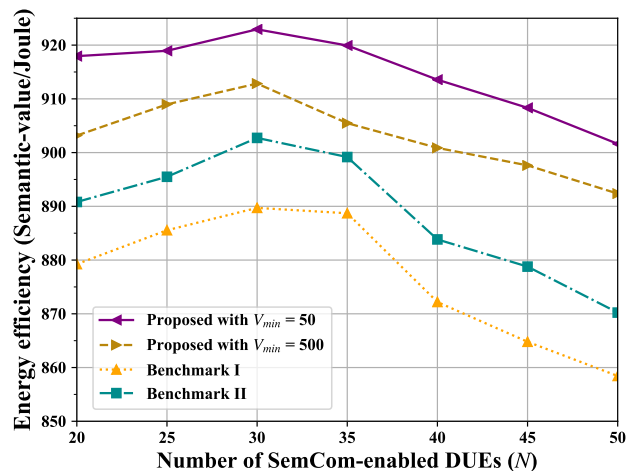


Fig. 6. Energy efficiency versus different numbers of DUEs.

to less allocated bandwidth dominates the trend of  $\eta_{EE}$ , even though each DUE can still have a better spectrum reusing option. Besides, the proposed solution with  $V_{min} = 500$  has a worse  $\eta_{EE}$  performance compared to that with  $V_{min} = 50$ . This can be explained by that  $V_{min} = 500$  represents the stringent constraints of (8a) and (8b) and thus results in a smaller feasible region of variables  $P^C$  and  $P^D$  in  $\mathbf{P0}$ , which incurs a deterioration of  $\eta_{EE}$  that can be achieved.

Next, we compare the proposed solution with the two benchmarks under varying number of DUEs (i.e.,  $N$ ) between 20 and 50 at the same two semantic value thresholds in Fig. 6. It is observed that the energy efficiency  $\eta_{EE}$  obtained by our solution still exceeds the benchmarks at each point with a significant performance gain. Likewise,  $\eta_{EE}$  becomes higher with  $N$  at the beginning, and then decreases when exceeding 30. The former phenomenon is because the performance gain on  $V^{total}$  resulted from the increase of  $N$  surpasses the impact of the power consumption increase on  $E^{total}$ . When  $N$  surpasses a maximum threshold (i.e.,  $N = 40$  in our case), such performance increase eventually reaches its peak and is saturated and even worse. This is because that the signal interference between spectrum-sharing links will dominate the reduction of  $\eta_{EE}$ , as more CUEs need to share their spectrum with the increase of the number of DUEs. Moreover, the higher number of DUEs indicates the more restrictive spectrum sharing optimization, which also brings a certain degree of performance limitation.

Apart from these, the impacts of the maximum allowable transmit power of CUEs (i.e.,  $P_{max}^C$ ) and DUEs (i.e.,  $P_{max}^D$ ) are tested in Fig. 7 and Fig. 8, respectively, where two differing numbers of SemCom services  $K = 20$  and  $K = 200$  are taken into account. First, it is seen in both figures that our proposed solution renders a better energy efficiency performance compared with the two benchmarks with the same  $K$ . In Fig. 7, as  $P_{max}^C$  rises from 18 to 24 dBm, an increase is observed by the proposed solution at both  $K$  curves and then eventually stabilized. This can be understood by that at the beginning, CUEs prefers to have a higher transmit power at the looser power constraint to obtain a better semantic value

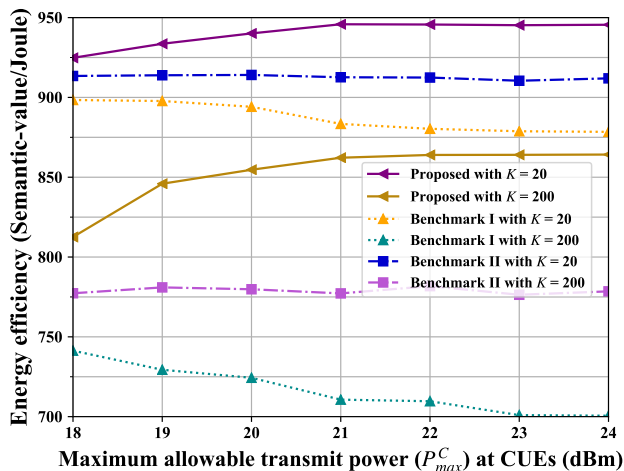


Fig. 7. Energy efficiency versus varying maximum transmit power of CUEs.

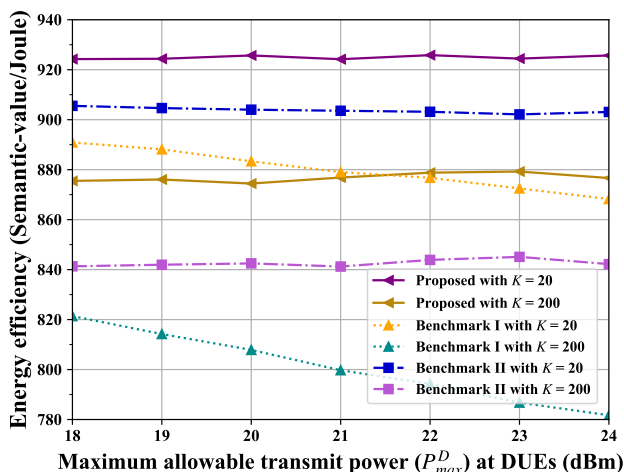
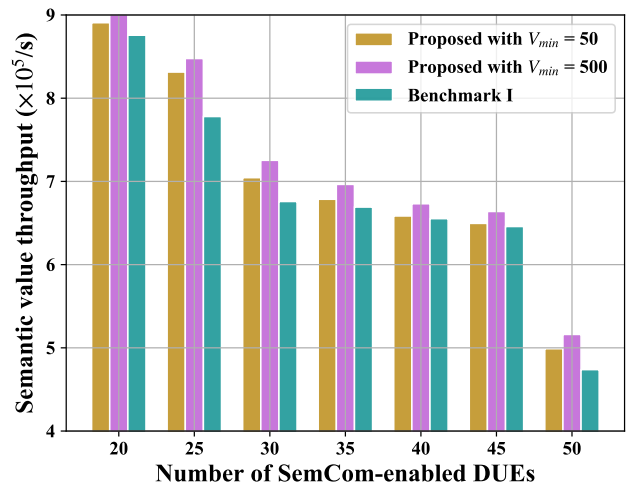
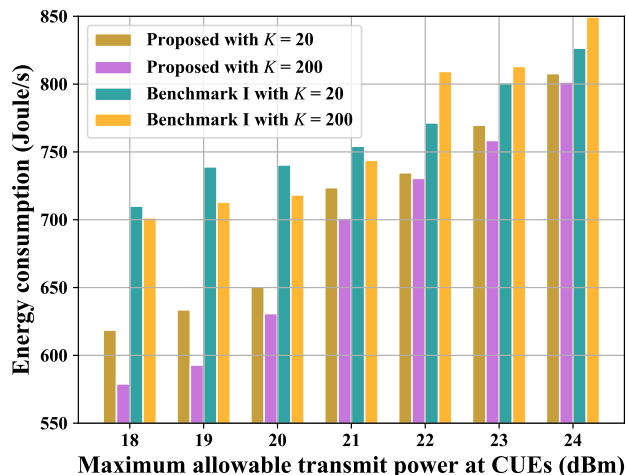


Fig. 8. Energy efficiency versus varying maximum transmit power of DUEs.

performance, especially for these CUEs without spectrum reusing. Afterward, when  $P^C_{max}$  keeps increasing, the optimal transmit power for these CUEs tends to be stable, as the further increasing of power will lead to more energy consumption and the worse  $\eta_{EE}$  performance. In addition, Fig. 8 depicts a steady trend as  $P^D_{max}$  grows when compared with Fig. 7 in the performance presentation of our solution. This is because the optimal transmit power for DUEs in our proposed solution should be in a small region to align with the corresponding minimum semantic value constraint  $V_{min}$ , and therefore, the increase of  $P^D_{max}$  will not affect the final  $\eta_{EE}$  performance. Furthermore, notice that in either Fig. 7 or Fig. 8, the energy efficiency of each of the three schemes with the smaller  $K$  is always higher than that with the larger one. This is due to the fact that a larger  $K$  implies less discrepancy in users' preferences for different SemCom services given the fixed skewness of Zipf distribution, and these services with low semantic value will become inevitably dominant, thereby causing the worse energy efficiency.

Finally, Fig. 9 and Fig. 10 demonstrate the semantic value throughput (i.e.,  $V^{total}$ ) under varying  $N$  with different  $V_{min}$  and the overall energy consumption (i.e.,  $E^{total}$ ) under varying

Fig. 9. Semantic value throughput ( $V^{total}$ ) versus different numbers of DUEs.Fig. 10. Overall energy consumption ( $E^{total}$ ) versus varying  $P^C_{max}$ .

$P^C_{max}$  with different  $K$ , respectively. It is first seen in Fig. 9 that  $V^{total}$  gradually drops as the increase of  $N$ , and the setting of  $V_{min} = 500$  leads to a better performance than  $V_{min} = 50$ . The former trend is because that the increase of  $N$  makes more CUEs share their spectrum that can cause greater signal interference and worse SINR to them, thus resulting in the decrease of overall bit throughput as well as overall semantic value. As for the latter phenomenon, this is relatively clear since  $V_{min} = 500$  sets a higher semantic value threshold for each CUE and DUE link that must be satisfied during our optimization process. Moreover, the semantic value observed by our solution always outperforms benchmark I at each point. This can be interpreted by that the benchmark I employs the maximum power allocation scheme, bringing very heavy interference burden on these CUEs and DUEs with spectrum sharing, which performance degradation outweighs the performance gain from the maximum power to those CUEs without spectrum sharing. As plotted in Fig. 10, an uptrend of  $E^{total}$  is observed for all resource allocation schemes as the growing of  $P^C_{max}$ . This result is expected because for these CUEs with no spectrum sharing, they prefer to perform

SemCom with their maximum allowable transmit power to maximize the achievable semantic value performance, since they have no concerns for signal interferences compared with these CUEs with spectrum sharing. Besides, it is noticed that the proposed solution with the larger  $K$  consumes less energy than that with the small  $K$ . This can be understood by that the larger  $K$  means the larger  $\theta_i^C$  and  $\theta_j^D$  in (3) and (4) from the statistical perspective, which represents the looser constraints for (8a) and (8b). As such, the smaller transmit power may be utilized by CUEs and DUEs to meet their minimum semantic value threshold, and thus leading to the less energy consumption. Again, the proposed solution achieves less energy consumption in comparison with benchmark I at each  $P_{max}^C$  setting for the same  $K$ , which is consistent with the previous results in Fig. 7 and proves the performance superiority of the proposed solution.

## V. CONCLUSIONS

In this paper, we have investigated the wireless resource allocation problem for energy efficiency maximization in the novel network scenario of D2D-SCN, where multiple CUEs and DUEs coexist for SemCom service provisioning. To measure the semantic information importance in SemCom, the user preference-aware semantic triplet transmission has been first introduced to identify the semantic value performance, while taking into account the power circuit consumption from the specific semantic encoding mechanism for energy efficiency. On this basis, a joint power control and spectrum reuse problem has been then formulated to maximize the energy efficiency of D2D-SCN. After the fractional-to-subtractive primal problem transformation and decomposition, we have developed a three-stage method to seek the optimal resource allocation solution with low computational complexity, and the solution optimality has been theoretically proved. Numerical results have verified the performance superiority of the proposed solution in terms of energy efficiency, semantic value, and energy consumption compared with differing benchmarks.

This work can serve as a pioneer in providing valuable insights for follow-up research on D2D SemCom underlying cellular networks. Other relevant networking issues in the D2D-SCN, such as cellular/D2D SemCom mode switching and semantic security-driven or user fairness-aware resource allocation, can treat this paper as the theoretical baseline for reference. Moreover, since this work is limited to only semantic-encoding based energy efficiency optimization under known SemCom service popularity, a further extension of D2D-SCN about simultaneously considering the energy loss of semantic decoding in the presence of unknown user semantic preferences could be our next potential research direction.

### APPENDIX A PROOF OF PROPOSITION 1

First let  $(\mathbf{P}^{C*}, \mathbf{P}^{D*}, \boldsymbol{\alpha}^*)$  and  $(\widehat{\mathbf{P}}^C, \widehat{\mathbf{P}}^D, \widehat{\boldsymbol{\alpha}})$  denote the optimal solution and an arbitrary feasible solution to **P0**,

respectively. Clearly, we have

$$\eta_{EE}^* = \frac{V^{total}(\mathbf{P}^{C*}, \mathbf{P}^{D*}, \boldsymbol{\alpha}^*)}{E^{total}(\mathbf{P}^{C*}, \mathbf{P}^{D*}, \boldsymbol{\alpha}^*)} \geq \frac{V^{total}(\widehat{\mathbf{P}}^C, \widehat{\mathbf{P}}^D, \widehat{\boldsymbol{\alpha}})}{E^{total}(\widehat{\mathbf{P}}^C, \widehat{\mathbf{P}}^D, \widehat{\boldsymbol{\alpha}})}. \quad (24)$$

It is not difficult to find that  $E^{total} > 0$  holds in any solution, the following conclusions can be easily derived from (24), i.e.,

$$V^{total}(\mathbf{P}^{C*}, \mathbf{P}^{D*}, \boldsymbol{\alpha}^*) - \eta_{EE}^* E^{total}(\mathbf{P}^{C*}, \mathbf{P}^{D*}, \boldsymbol{\alpha}^*) = 0, \quad (25)$$

and

$$V^{total}(\widehat{\mathbf{P}}^C, \widehat{\mathbf{P}}^D, \widehat{\boldsymbol{\alpha}}) - \eta_{EE}^* E^{total}(\widehat{\mathbf{P}}^C, \widehat{\mathbf{P}}^D, \widehat{\boldsymbol{\alpha}}) \leq 0. \quad (26)$$

Note that **P0** and **P1** have the same feasible region as they have the identical constraints (8a)-(8g), if given  $\eta_{EE}^*$  as the input of the objective function in **P1**, it is obviously seen from (25) and (26) that the achievable maximum objective value of  $F(\eta_{EE}^*)$  in **P1** must be 0, and its optimal solution is exactly the optimal solution to **P0**, i.e.,  $(\mathbf{P}^{C*}, \mathbf{P}^{D*}, \boldsymbol{\alpha}^*)$ .

Meanwhile, considering the other two remaining cases of  $F(\eta_{EE}) > 0$  and  $F(\eta_{EE}) < 0$  in **P1**, and let  $(\overline{\mathbf{P}}^{C*}, \overline{\mathbf{P}}^{D*}, \overline{\boldsymbol{\alpha}}^*)$  and  $(\widetilde{\mathbf{P}}^{C*}, \widetilde{\mathbf{P}}^{D*}, \widetilde{\boldsymbol{\alpha}}^*)$  be their optimal solutions to **P1** respectively, then we have

$$V^{total}(\overline{\mathbf{P}}^{C*}, \overline{\mathbf{P}}^{D*}, \overline{\boldsymbol{\alpha}}^*) - \eta_{EE} E^{total}(\overline{\mathbf{P}}^{C*}, \overline{\mathbf{P}}^{D*}, \overline{\boldsymbol{\alpha}}^*) > 0, \quad (27)$$

and

$$V^{total}(\widetilde{\mathbf{P}}^{C*}, \widetilde{\mathbf{P}}^{D*}, \widetilde{\boldsymbol{\alpha}}^*) - \eta_{EE} E^{total}(\widetilde{\mathbf{P}}^{C*}, \widetilde{\mathbf{P}}^{D*}, \widetilde{\boldsymbol{\alpha}}^*) < 0. \quad (28)$$

Again leveraging  $E^{total} > 0$ , given any  $\eta_{EE}$ , (27) yields

$$\frac{V^{total}}{E^{total}} = \eta_{EE} < \frac{V^{total}(\overline{\mathbf{P}}^{C*}, \overline{\mathbf{P}}^{D*}, \overline{\boldsymbol{\alpha}}^*)}{E^{total}(\overline{\mathbf{P}}^{C*}, \overline{\mathbf{P}}^{D*}, \overline{\boldsymbol{\alpha}}^*)}, \quad (29)$$

and likewise, (28) yields

$$\frac{V^{total}}{E^{total}} = \eta_{EE} > \frac{V^{total}(\widetilde{\mathbf{P}}^{C*}, \widetilde{\mathbf{P}}^{D*}, \widetilde{\boldsymbol{\alpha}}^*)}{E^{total}(\widetilde{\mathbf{P}}^{C*}, \widetilde{\mathbf{P}}^{D*}, \widetilde{\boldsymbol{\alpha}}^*)}. \quad (30)$$

From (29) and (30), it can be concluded that for any feasible solution to **P0**, it must not be the optimal solution to **P1** when  $F(\eta_{EE}^*) \neq 0$ . This completes the proof.

### APPENDIX B PROOF OF PROPOSITION 2

This proposition can be proved by using contradiction. According to all constraints of **P2** <sub>$i,j$</sub> , if the optimization problem is supposed to be solvable, the optimal power allocation solution  $(P_i^{C*}, P_j^{D*})$  must fall into the non-empty  $\psi$ . Here, we first assume that  $(P_i^{C*}, P_j^{D*})$  is not the coincide point of the two line segments while making  $\widetilde{\lambda}_1(P_j^D)$  and  $\widetilde{\lambda}_2(P_i^C)$  simultaneously reach their respective maxima, i.e.,

$$(P_i^{C*}, P_j^{D*}) \notin \left\{ \left( \overleftarrow{P}_i^C, \overleftarrow{P}_j^D \right) \mid \left( \overleftarrow{P}_i^C, \overleftarrow{P}_j^D \right) = \left( \overrightarrow{P}_i^C, \overrightarrow{P}_j^D \right) \in \psi \right\}. \quad (31)$$

This means that  $(P_i^{C*}, P_j^{D*})$  should not be the optimal point for at least one line segment w.r.t.  $\tilde{\lambda}_1(P_j^D)$  or w.r.t.  $\tilde{\lambda}_2(P_i^C)$ . For illustration, let  $\tilde{l}$  denote the line segment through  $(P_i^{C*}, P_j^{D*})$ .

However, it is also noticed that  $\psi$  must be a closed and bounded region in one of the three cases in Fig. 3. Due to the convex property of  $\tilde{\lambda}_1(P_j^D)$  or  $\tilde{\lambda}_2(P_i^C)$ , there must be another point  $(\overline{P}_i^C, \overline{P}_j^D)$  on the same line segment  $\tilde{l}$ , leading to a larger value  $\tilde{\lambda}_1(P_j^D)$  or w.r.t.  $\tilde{\lambda}_2(P_i^C)$ . That is, one of the following cases must exist:

$$\tilde{\lambda}_1(\overline{P}_j^D) > \tilde{\lambda}_1(P_j^{D*}) \quad \text{or} \quad \tilde{\lambda}_2(\overline{P}_i^C) > \tilde{\lambda}_2(P_i^{C*}). \quad (32)$$

Meanwhile, since  $(P_i^{C*}, P_j^{D*})$  and  $(\overline{P}_i^C, \overline{P}_j^D)$  are on the same line segment, this leads to another fact that  $\sigma_i^C r_i^C$  (in the left case of (32)) or  $\sigma_j^D r_j^D$  (in the right case of (32)) gets the same value at the two points. Combined with (12), clearly, either of the cases contradicts the assumption that  $(P_i^{C*}, P_j^{D*})$  is the optimal solution in  $\psi$ . This completes the proof.

## REFERENCES

- [1] P. Zhang, W. Xu, H. Gao, K. Niu, X. Xu, X. Qin, C. Yuan, Z. Qin, H. Zhao, J. Wei, *et al.*, "Toward wisdom-evolutionary and primitive-concise 6G: A new paradigm of semantic communication networks," *Engineering*, vol. 8, no. 1, pp. 60–73, 2022.
- [2] Y. Sun, L. Zhang, L. Guo, J. Li, D. Niyato, and Y. Fang, "S-RAN: Semantic-aware radio access networks," *IEEE Communications Magazine*, pp. 1–7, 2024.
- [3] H. Xie, Z. Qin, G. Y. Li, and B.-H. Juang, "Deep learning enabled semantic communication systems," *IEEE Transactions on Signal Processing*, vol. 69, pp. 2663–2675, 2021.
- [4] G. Shi, Y. Xiao, Y. Li, and X. Xie, "From semantic communication to semantic-aware networking: Model, architecture, and open problems," *IEEE IEEE Communications Magazine*, vol. 59, no. 8, pp. 44–50, 2021.
- [5] L. Xia, Y. Sun, C. Liang, D. Feng, R. Cheng, Y. Yang, and M. A. Imran, "WiserVR: Semantic communication enabled wireless virtual reality delivery," *IEEE Wireless Communications*, vol. 30, no. 2, pp. 32–39, 2023.
- [6] L. Xia, Y. Sun, C. Liang, L. Zhang, M. A. Imran, and D. Niyato, "Generative AI for semantic communication: Architecture, challenges, and outlook," *arXiv preprint arXiv:2308.15483*, 2023.
- [7] H. Xie and Z. Qin, "A lite distributed semantic communication system for Internet of Things," *IEEE Journal on Selected Areas in Communications*, vol. 39, no. 1, pp. 142–153, 2020.
- [8] Z. Weng and Z. Qin, "Semantic communication systems for speech transmission," *IEEE Journal on Selected Areas in Communications*, vol. 39, no. 8, pp. 2434–2444, 2021.
- [9] Y. Jiang, Y. Zou, H. Guo, T. A. Tsiftsis, M. R. Bhatnagar, R. C. de Lamare, and Y.-D. Yao, "Joint power and bandwidth allocation for energy-efficient heterogeneous cellular networks," *IEEE Transactions on Communications*, vol. 67, no. 9, pp. 6168–6178, 2019.
- [10] L. Yan, Z. Qin, R. Zhang, Y. Li, and G. Y. Li, "Resource Allocation for Text Semantic Communications," *IEEE Wireless Communications Letters*, 2022.
- [11] H. Zhang, H. Wang, Y. Li, K. Long, and A. Nallanathan, "DRL-driven dynamic resource allocation for task-oriented semantic communication," *IEEE Transactions on Communications*, vol. 71, no. 7, pp. 3992–4004, 2023.
- [12] N. H. Sang, N. D. Hai, N. D. D. Anh, N. C. Luong, V.-D. Nguyen, S. Gong, D. Niyato, and D. I. Kim, "Wireless power transfer meets semantic communication for resource-constrained IoT networks: A joint transmission mode selection and resource management approach," *IEEE Internet of Things Journal*, pp. 1–1, 2024.
- [13] L. Xia, Y. Sun, D. Niyato, L. Zhang, and M. A. Imran, "Wireless Resource Optimization in Hybrid Semantic/Bit Communication Networks," *IEEE Transactions on Communications*, 2024.
- [14] J. Su, Z. Liu, Y.-a. Xie, K. Ma, H. Du, J. Kang, and D. Niyato, "Semantic communication-based dynamic resource allocation in D2D vehicular networks," *IEEE Transactions on Vehicular Technology*, vol. 72, no. 8, pp. 10784–10796, 2023.
- [15] Z. Yang, M. Chen, Z. Zhang, and C. Huang, "Energy Efficient Semantic Communication Over Wireless Networks With Rate Splitting," *IEEE Journal on Selected Areas in Communications*, vol. 41, no. 5, pp. 1484–1495, 2023.
- [16] L. Xia, Y. Sun, D. Niyato, D. Feng, L. Feng, and M. A. Imran, "xURLLC-aware service provisioning in vehicular networks: A semantic communication perspective," *IEEE Transactions on Wireless Communications*, vol. 23, no. 5, pp. 4475–4488, 2024.
- [17] S. Yang, J. Tian, H. Zhang, J. Yan, H. He, Y. Jin *et al.*, "TransMS: Knowledge graph embedding for complex relations by multidirectional semantics," in *IJCAI*, 2019, pp. 1935–1942.
- [18] X. Chen, S. Jia, and Y. Xiang, "A review: Knowledge reasoning over knowledge graph," *Expert Systems with Applications*, vol. 141, no. 5, p. 112948, 2020.
- [19] S. Gao, X. Qin, L. Chen, Y. Chen, K. Han, and P. Zhang, "Importance of semantic information based on semantic value," *IEEE Transactions on Communications*, 2024.
- [20] L. Xia, Y. Sun, D. Niyato, X. Li, and M. A. Imran, "Joint user association and bandwidth allocation in semantic communication networks," *IEEE Transactions on Vehicular Technology*, pp. 1–13, 2023.
- [21] S. T. Piantadosi, "Zipf's word frequency law in natural language: A critical review and future directions," *Psychonomic Bulletin & Review*, vol. 21, pp. 1112–1130, 2014.
- [22] N. B. Hassine, D. Marinca, P. Minet, and D. Barth, "Popularity prediction in content delivery networks," in *2015 IEEE 26th Annual International Symposium on Personal, Indoor, and Mobile Radio Communications (PIMRC)*. IEEE, 2015, pp. 2083–2088.
- [23] G. Li, J. Wu, J. Li, K. Wang, and T. Ye, "Service popularity-based smart resources partitioning for fog computing-enabled industrial Internet of Things," *IEEE Transactions on Industrial Informatics*, vol. 14, no. 10, pp. 4702–4711, 2018.
- [24] S. Guo, Y. Shi, Y. Yang, and B. Xiao, "Energy efficiency maximization in mobile wireless energy harvesting sensor networks," *IEEE Transactions on Mobile Computing*, vol. 17, no. 7, pp. 1524–1537, 2017.
- [25] D. W. K. Ng, E. S. Lo, and R. Schober, "Energy-efficient resource allocation in OFDMA systems with large numbers of base station antennas," *IEEE Transactions on Wireless Communications*, vol. 11, no. 9, pp. 3292–3304, 2012.
- [26] Z. Q. Liew, Y. Cheng, W. Y. B. Lim, D. Niyato, C. Miao, and S. Sun, "Economics of semantic communication system in wireless powered Internet of Things," in *ICASSP 2022-2022 IEEE International Conference on Acoustics, Speech and Signal Processing (ICASSP)*. IEEE, 2022, pp. 8637–8641.
- [27] G. Auer, V. Giannini, C. Desset, I. Godor, P. Skillermark, M. Olsson, M. A. Imran, D. Sabella, M. J. Gonzalez, O. Blume *et al.*, "How much energy is needed to run a wireless network?" *IEEE Wireless Communications*, vol. 18, no. 5, pp. 40–49, 2011.
- [28] W. Dinkelbach, "On nonlinear fractional programming," *Management Science*, vol. 13, no. 7, pp. 492–498, 1967.
- [29] D. B. West *et al.*, *Introduction to Graph Theory*. Prentice hall Upper Saddle River, 2001, vol. 2.
- [30] J. Edmonds and R. M. Karp, "Theoretical improvements in algorithmic efficiency for network flow problems," *Journal of the ACM (JACM)*, vol. 19, no. 2, pp. 248–264, 1972.
- [31] Q. Wang, M. Hempstead, and W. Yang, "A realistic power consumption model for wireless sensor network devices," in *2006 3rd Annual IEEE Communications Society on Sensor and ad-hoc Communications and Networks*, vol. 1, pp. 286–295, 2006.
- [32] P. Pawar and A. Trivedi, "Joint uplink-downlink resource allocation for D2D underlaying cellular network," *IEEE Transactions on Communications*, vol. 69, no. 12, pp. 8352–8362, 2021.
- [33] H. Esmat, M. M. Elmesalawy, and I. Ibrahim, "Uplink resource allocation and power control for D2D communications underlaying multi-cell mobile networks," *AEU-International Journal of Electronics and Communications*, vol. 93, pp. 163–171, 2018.
- [34] C. Guo, L. Liang, and G. Y. Li, "Resource allocation for vehicular communications with low latency and high reliability," *IEEE Transactions on Wireless Communications*, vol. 18, no. 8, pp. 3887–3902, 2019.
- [35] T.-S. Kim and S.-L. Kim, "Random power control in wireless ad hoc networks," *IEEE Communications Letters*, vol. 9, no. 12, pp. 1046–1048, 2005.
- [36] D. D. Ningombam and S. Shin, "Non-orthogonal resource sharing optimization for D2D communication in LTE-A cellular networks: A

fractional frequency reuse-based approach," *Electronics*, vol. 7, no. 10, p. 238, 2018.